

Design of Wireless Power Supply Optimized Structure for Capsule Endoscopes

Chang Cui^a, Qiang Zhao^{a,*}, Zhongjian Li^b

^aDepartment of Information and Control Engineering, Liaoning Shihua University, Liaoning Fushun, 113001, China;

^bSchool of Science, University of Southern Queensland, Toowoomba, Australia;

Abstract

Wireless power transmission is an important method for powering wireless capsule endoscopes, but its efficiency is low, especially when the devices move freely in random positions and orientations. To improve the stability and efficiency of the endoscope in vivo, this study designed an optimization method for planar spiral coils utilized in wireless power transfer for capsule endoscopes. An optimized structure using six planar spiral coils was first proposed as the transmitting coil, and the efficiency of a series-parallel wireless power transmission model was analyzed. A theoretical model was then examined for the magnetic field vector distributions of the spiral-type transmitting coil by using an elliptic coordinate system. The relationship between the position of the receiving coil and the coupling coefficient was determined when the position and attitude changed. Finally, the experimental device of the wireless power supply system of the endoscope was designed with a class-E amplifier and Liz coil. The simulation and experimental results showed that the proposed method can generate high intensity magnetic field uniform, which can improve the efficiency of the wireless power transmission in the case of axial deviation and angular misalignment. The experimental results also indicated that the proposed scheme can meet the needs of the power supply of wireless endoscopes.

Keywords: wireless power transmission; wireless capsule endoscopes; spiral-type coil antenna; magnetic coupling; magnetic field vector

1. Introduction

In the examination of gastrointestinal diseases, the diagnostic modality of capsule endoscopes is accurate, convenient, and comfortable to use, and it has therefore become superior to conventional endoscopes [1, 2]. The capsule endoscope is powered by cell batteries or cables when they operate in the human body. However, the problem in the supply of sufficient amount of power confines the clinical application of capsule endoscopes [3]. Wireless power supply technology is considered the primary choice in solving this problem [4]. In wireless capsule endoscopes, the barrier between the body organs and blood, as well as the distance between the receiving and transmitting coils cause exceedingly low efficiency in the energy supply. If the position and posture of the endoscope are changed, then the coupling degree of the transmitting and receiving ends may be subject to change at any time. This circumstance is an important reason for the low efficiency of the system. To address these problems, an optimized magnetic coupling model and proper coil structure are required to deliver both a good match and

high transmission efficiency when the position and attitude of the receiving end are changed.

2. State of the art

The earliest application of a transcutaneous energy transmission system, which is a magnetic coupling wireless power supply scheme, was first realized in the wireless power supply technology of wireless endoscopes. As early as the 1970s, scientists studied transcutaneous energy transmission system through animal experiments. In a six-month trial, the transcutaneous energy transfer system did not significantly affect the physiological condition of the experimental animals, and the transmission efficiency of the system generally reached more than 90% [5]. However, the transcutaneous energy transfer system is inappropriate for micro devices used for the human body because the receive coil volume is exceedingly large and the transmission distance is extremely small. Therefore, this system can be applied only in heart pacemakers and other implantable medical devices.

Owing to the distance between the digestive tract and the diagnostic device in the receiving coil, a transmitting coil is usually more than 20 cm. Furthermore, capsule endoscopes

*Corresponding author

Email address: 1nshzq@126.com (Qiang Zhao)

need to be swallowed, thereby strictly limiting the volume of the receiving end [6]. The attitude and position of the device change with the peristalsis of the intestinal peristalsis, and the coupling degree between the transmitter and receiver is also subject to change at any time [7].

With respect to the problem of the changing attitude in wireless endoscopes a three-dimensional receiving coil can overcome the influence of the coupling degree of the coil in the body [8]. R. Puers, et al. designed a three-dimensional receiving coil structure for the special working environment of wireless endoscopes. Experimental results showed that the energy is stable at 300 mW [9]. Bert Lenaerts and Robert Puers also conducted a study on a three-dimensional coil in which the receiver can receive energy of 150 mW [10].

Minh Quoc Nguyen, et al. examined in detail the positional and angular misalignment analysis for circular transmitter antennas [11]. Recent studies showed that the use of spiral structures for transmitter antennas can significantly improve wireless power transmission and can provide a satisfactory beam size for the receiver antenna [12]. Minh Quoc Nguyen, et al. developed a mathematical model to analyze near-field distributions and optimize the designs of spiral coils to achieve maximum power transfer and system efficiency [13]. A method of wireless power transmission based on electromagnetic localization and synthesis of the magnetic field vector was proposed [14]. The capsule endoscopy receiver is always moving through the gastrointestinal tract, which degrades transfer efficiency due to variations in the distance, angle, and axial misalignment. But in [14], the transmitting coil was composed of a cylindrical spiral coil that yields a low coupling coefficient. Some researchers improved wireless power transfer efficiency using a ceramic filled cavity [15]. Nonetheless, the system remained inappropriate under varying conditions. Hence, a wireless power transfer system for biomedical capsule endoscopy application must include additional methods to maintain strong transfer efficiency under these dynamic circumstances. In previous research [16–18] an efficiency improvement was demonstrated with a symmetric coil wireless power transfer system.

The remainder of this paper is organized into five sections. Following the Introduction, Section 2 describes the traditional power supply for the endoscope power transmission system. Section 3 presents the modeling and system stability analysis of a wireless endoscope system and a new method of three pairs of transmitting coils. Section 4 shows how the proposed work was verified using measured experimental results and the analysis of the effects on the transfer efficiency of WTP system. Two different methods were selected to optimize power transfer while receiving coil movement. Section 5 summarizes the research conclusions.

3. Methodology

3.1. Modeling and analysis of wireless endoscope system

In the wireless endoscope power supply system, the receiving coil in the human digestive tract moves continuously,

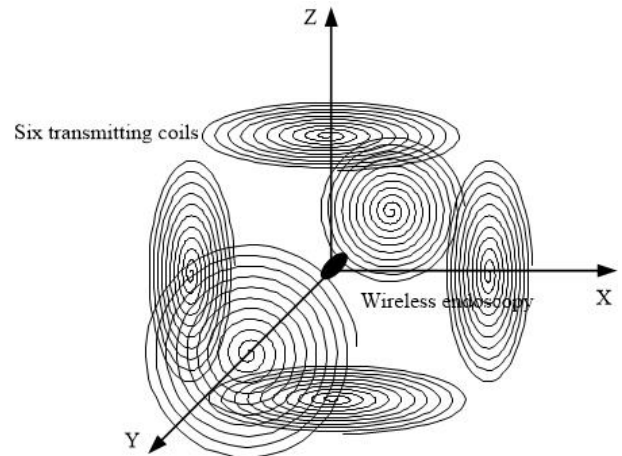


Figure 1: Spiral coil antenna configuration

resulting in constant changes in its position and attitude in the magnetic field. To obtain stable energy, an appropriate approach for overcoming the problems caused by the attitude and position of the receiver should be determined.

In this study, a transmitting and receiving coil is used which includes a Helmholtz coil with spiral structures, as shown in Fig. 1. This coil can generate a uniform magnetic field, can significantly improve wireless power transmission, and has an adequate beam size for the receiver antenna. These devices consist of two identical circular coils placed symmetrically on either side of the experimental area along a common axis and are separated by a distance equal to the radius of the coil. If a pair of the same current-carrying circular coil and coaxial exists and is parallel to each other in the same direction current when the coil spacing is equal to the radius of coil, the total magnetic field of the current-carrying coil near the halfway point of the axis of a wide range is uniform. The space of the Helmholtz coil is open and easy to use. This coil demonstrates a good linear relationship between the magnetic field and current. The space of the magnetic field is an extremely wide uniform area suitable for one-dimensional, two-dimensional and three-dimensional space combination magnetic fields. The electromagnetic distribution characteristic of a Helmholtz coil structure is applicable to the wireless endoscope energy supply system.

Improving the quality factor of the coil in the resonant power supply system is an effective method for improving transmission efficiency. The loss of the circuit is small when the Q value of the coil is high. The Q value of the coil is related to the DC resistance of the conductor, the dielectric loss of the skeleton, the loss caused by the shield or the iron core, and the influence of the high frequency skin effect. Owing to the skin and proximity effects of the coil, the AC resistance of the coil increases rapidly with the increase in frequency. Therefore, the main scheme is to reduce the skin and proximity effects of the coil as well as the AC resistance. At the same voltage, the current value of the coil is increased, and the current intensity is proportional to the magnetic field strength of the coil.

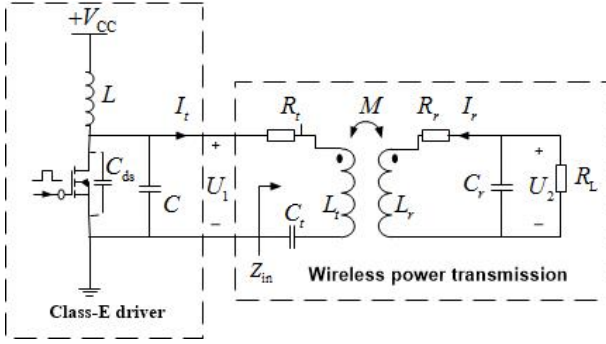


Figure 2: Series-parallel compensation topologies of coupling circuits

According to $Q = \omega L/R$, coil inductance should be increased or the resistance of the coil should be reduced when the quality factor of the coil needs to be improved. Inductance is related to the diameter and length of the coil. The Q value of the coil, which varies from tenths to hundredths, is reduced, and its stability is poor because of the distributed capacitance. As such, the distributed capacitance of the coil should be as small as possible. To reduce impedance and retain the same inductance, the Litz line scheme is used in the high frequency design to replace the single stranded wire. This scheme can reduce the skin effect of the coil while the Q value of the coil increases, and it can simultaneously improve coupling efficiency and transmission power.

Fig. 2 illustrates the series-parallel compensation topologies using class-E.

The transmitter coil L_t and tuning capacitor C_t are connected in series, which can improve the power transfer significantly by fine tuning. The receiver coil L_r is connected in parallel with the tuning capacitor C_r to stabilize the voltage and reduce the noise and harmonics from the nonlinear class-E amplifier in the transmitter circuit. From the coupling circuits, Formula (1) can be obtained.

$$\begin{bmatrix} V_t \\ 0 \end{bmatrix} = \begin{bmatrix} Z_t & -j\omega M \\ -j\omega M & Z_r \end{bmatrix} \begin{bmatrix} I_t \\ I_r \end{bmatrix} \quad (1)$$

Z_t and Z_r are the impedance of transmit and receive circuits depicted in Formulas (2) and (3), respectively.

$$Z_t = R_t + j(\omega L_t - \frac{1}{\omega C_t}) \quad (2)$$

$$Z_r = R_r + j\omega L_r + \frac{R_L}{1 + j\omega C_r R_L} \quad (3)$$

From Formulas (1), (2), and (3), we can obtain Formula (4).

$$\begin{bmatrix} I_t \\ I_r \end{bmatrix} = \frac{1}{Z_t Z_r + \omega^2 M^2} \begin{bmatrix} Z_r & j\omega M \\ j\omega M & Z_t \end{bmatrix} \begin{bmatrix} V_t \\ 0 \end{bmatrix} \quad (4)$$

When $\omega L_t - 1/\omega C_t = 0$ and $\omega L_r - 1/\omega C_r = 0$, the value of transmission efficiency μ is at a maximum when the transmitter and receiver are resonant. In the following analysis, with the use of coil quality factor Q , the performance of the coil is

represented by coil inductance L , and coupling coefficient k denotes mutual inductance M as shown below.

$$Q = \frac{\omega L}{R}, k = \frac{M}{\sqrt{L_t L_r}} \Rightarrow L = \frac{QR}{\omega}, M = k \sqrt{L_t L_r} \quad (5)$$

The ratio of load resistance and receiving coil winding resistance is defined as the load factor.

$$\alpha = \frac{R_L}{R_r} \quad (6)$$

The transmission efficiency of the compensation topology can be expressed as follows:

$$\eta = \frac{\alpha k^2 Q_t Q_r (1 + k^2 Q_t Q_r + Q_r^2)}{(\alpha + 1 + k^2 Q_t Q_r + Q_r^2)(\alpha + \alpha k^2 Q_t Q_r + 1 + k^2 Q_t Q_r + Q_r^2)} \quad (7)$$

where, Q_t and Q_r are the transmitting and receiving coils quality factor

From Formula (7), the coupling efficiency of the system is determined by the load factor α and $k^2 Q_t Q_r$. By derivation, when the series-parallel compensation topology load factor α satisfies the following conditions:

$$\alpha = \frac{1 + k^2 Q_t Q_r + Q_r^2}{\sqrt{1 + k^2 Q_t Q_r}} \quad (8)$$

The system maximum coupling efficiency is

$$\eta_{\max} = \frac{k^2 Q_t Q_r}{(1 + \sqrt{1 + k^2 Q_t Q_r})^2} \quad (9)$$

The analysis in the preceding paragraph implies that when the circuit achieves maximum efficiency, α refers to Q_t square when the matching capacitor is adjusted to the resonant state. This observation suggests that the load impedance is Q_r square times the resonant impedance of the receiver.

3.2. System stability analysis

The distance between the transmitting and receiving coils is large, which greatly reduces the electromagnetic coupling efficiency of the system. To reduce the energy loss and improve the receiving power, two coils should be made in the frequency resonance state. Attitude, position, and frequency stabilities are problems relating to the stability of the wireless endoscope power supply. The physical connotation of stability refers to the ratio of the minimum and maximum powers to the energy receiving device, which is determined by the emission power.

$$W = \frac{P_{\min}}{P_{\max}} \quad (10)$$

In Formula (10), W is the stability of the energy transmission, P_{\min} is received at the receiving end of the minimum power, and P_{\max} is the maximum power.

Position stability is a problem relating to the relative position between the transmitting and receiving coils. Owing to the difference in the size of these coils, the position of

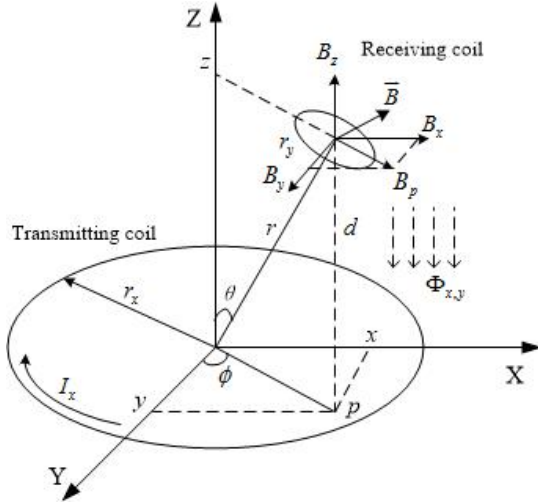


Figure 3: Magnetic field vector by a circular electrical current

$$\begin{cases} B_x = B_p \sin \phi \\ B_y = B_p \cos \phi \\ B_z = B_z \end{cases} \quad (12)$$

In the z axis direction, with an angle of θ to the z axis, the magnetic flux density component is denoted as follows:

$$B_\theta = |B_p \sin \theta + B_z \cos \theta| \quad (13)$$

On the z axis where $p = 0$, the components become $B_x = 0$, $B_y = 0$. Fig. 3 presents the vertical displacement d and the angle θ between the transmitting loop surface plane and the plane parallel to the receiving loop. The Biot-Savart law stipulates that the magnetic flux density B_z is at a field point r (at height above the center of the loop axis) induced by the loop.

$$B_z = \int dB_x = \frac{\mu_0 I_x}{4\pi} \int \frac{dl \times r}{|r|^3} \cos \theta = \frac{\mu_0 I_x r_x^2}{2(r_x^2 + d^2)^{3/2}} \quad (14)$$

where $I_x dl$ is the infinitesimal current source line on the transmitting loop, and μ_0 is the permeability of the free space. Faraday's and Lenz's laws imply that a time-varying current in the loop (I_x) results in a time variation of the magnetic flux through the receiving loop (Φ_z). The minus sign in (14) indicates that the electromagnetic field is in such a direction to produce a current whose flux reduces the magnitude of the electromagnetic field.

$$\varepsilon_z = -\frac{d\Phi_z}{dt} = -\frac{d}{dt} \int_S B_z ds = -M \frac{dI_x}{dt} \quad (15)$$

where ds is the infinitesimal surface area element defined by the transmitting loop, and M is the mutual inductance between coils. M can be obtained with Formula (17).

$$\begin{cases} dl_x = r_x d\phi \\ dl_y = r_y d\theta \\ r = \sqrt{r_x^2 + r_y^2 + d^2 + p^2 - 2pr_x \cos \theta + 2pr_y \cos \phi - 2r_x r_y \cos(\phi - \theta)} \end{cases} \quad (16)$$

$$M_L(r_x, r_y, d, p) = \frac{\mu_0 r_x r_y}{4\pi} \oint d\phi \oint \frac{\cos \theta}{r} d\theta \quad (17)$$

Combining (5), (16), and (17) creates a new expression in geometric terms (coil radii r_x and r_y , vertical displacement factor d , and angle θ) for the coupling coefficient.

$$k_{xy} = \frac{\mu_0 \pi r_x^2 r_y^2 \cos \theta}{2 \sqrt{L_x L_y} (r_x^2 + d^2)^{3/2}} \quad (18)$$

In the FEKO simulation, the electromagnetic field distribution of the transmitting coil in 1 MHz is shown in Fig. 4.

As indicated in Fig. 4, the inner area of the coil is brighter than its outer peripheral area. This observation implies that the magnetic field intensity in the central area of the coil is stronger than that in its outside part, and has a relatively uniform magnetic field distribution.

the receiving coil is constantly changing in the magnetic field of the transmitting coil. The coupling efficiency of the coil is mainly determined by the coupling coefficient k . Hence, the efficiency is closely related to the position of the two coils. To improve the efficiency of power transmission, the mutual inductance between the power-transmitting coil and the power-receiving coil should be increased. Once the relative position of the coils is changed, the coupling relationship between these coils will display an uncertainty, which may lead to the instability of the receiving terminal. To produce the optimal magnetic field vector vertical to the transverse surface of the power-receiving coil, the power-receiving coil needs to be localized.

Fig. 3 illustrates a simplified resonator model pair of single-turn loops with radii r_x and r_y ($r_x \gg r_y$). The field distributions of this model can then be derived from field superposition generated by loop currents. The simplified model allows for the rapid estimation of the power distribution of similar spiral coils. The electrical current is assumed uniformly distributed through the loop; hence, the magnetic flux density at any point in three-dimensional space in a cylindrical coordinate system (p, ϕ, z) can be expressed as below.

$$\begin{cases} B_p = \frac{\mu_0 I}{2\pi} \frac{z}{p[(r_x+p)^2+z^2]^{1/2}} \\ \quad \times \left[-K(k) + \frac{r_x^2+p^2+z^2}{(r_x-p)^2} E(k) \right] \\ B_\phi = 0 \\ B_z = \frac{\mu_0 I}{2\pi} \frac{1}{[(r_x+p)^2+z^2]^{1/2}} \\ \quad \times \left[K(k) + \frac{r_x^2-p^2-z^2}{(r_x-p)^2+z^2} E(k) \right] \end{cases} \quad (11)$$

where $k = 4\rho R/((\rho + R)^2 + z^2)$, $K(k)$, and $E(k)$ represents the complete elliptical integrals of the first and second types of the modulus.

In the Cartesian coordinate system, after the position and orientation angles of the power-receiving coil (x, y, z, θ, ϕ) are identified, the magnetic flux density component can be expressed as

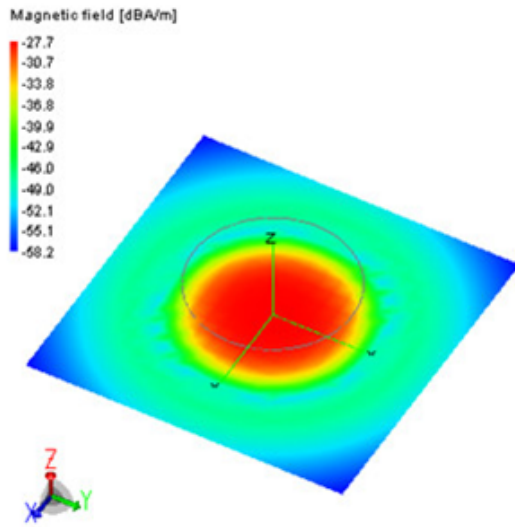


Figure 4: Electromagnetic field distribution of Helmholtz coil in 1 MHz

Fig. 5 shows the simulation analysis of the magnetic field of a planar spiral coil. Fig. 5a illustrates an energy incident schematic diagram, and Fig. 5b, c, and d show the magnetic field distributions of the transmitting coil at the resonant frequency. When $f_0 = 1.7$ MHz, $f_1 = 1.68$ MHz, and $f_2 = 1.72$ MHz, the magnetic field strength of the coil along the z and x axes in different directions is compared, as shown in Fig. 5e and f. Along the radial distribution of energy transfer, the magnetic field intensity generated by the resonance frequency signal is significantly larger than that of the non-resonant frequency. The magnetic field intensity of the energy transfer direction component along the axial distribution is the same. The plane spiral coil excited by the natural resonance frequency can generate the highest magnetic field intensity, implying that the transmitting and receiving coils can be used as a resonant body.

4. Result analysis and discussion

Fig. 6 shows the wireless power supply experimental device for endoscopes designed by the authors.

The transmitter and receiver coils are made in the form of magnetic resonance structures, and the coils are of spiral structures with Litz wires. A class-E amplifier is used to generate a high frequency power supply to directly connect to the transmitter coil. The receiver coil is connected to a resistive load. Table 1 lists the parameters of the transmitter, receiver coils, and other components.

In the experiment, two methods of coil structure are used for measurements. Method 1 is the single transmitting coil, and method 2 is the three pairs of transmitting coils. The efficiency of wireless transmission of these methods is compared. The transmitting and receiving coils in method 2 are the same as those in method 1. In method 2, each coil carries an equal current flowing in the same direction and

Table 1: Transmitter and receiver coil parameters

Parameters	Transmitter coil	Receiver coil
Number of strands	200	1
Wire diameter, mm	1	0.09
Inner radius, mm	130	8.2
Outer radius, mm	220	10
Turn number	50	600
Inductance, μH	56	2650
Capacitance, pF	Adjustable	3.3
Resistance, Ω	65	49
Load resistance, k Ω	2.7	
Frequency, MHz	1.7	

phase. The spacing between each pair of the coil is 25 cm, and six coils form a cube space. The receiving coil can move freely in space.

Measurements are carried out to observe the effects of the change in frequency (f), axial deviation (x , y , and z), angular misalignment between the vertical axes of the transmitting and receiving coils (θ), and load resistance (R_L). Formula (12) indicates that these parameters affect the coupling coefficient k . With variable parameters, the efficiency η can be optimized using method 2, and all measurement results are discussed below.

4.1. Frequencies-efficiency

In method 1, the receiving coil is on the center axis of the transmitting coil, and the distance is 12.5 cm. In method 2, the receiving coil is at the center of the six coils, and the distance from the bottom transmitting coils is 12.5 cm. Fig. 7a shows the relationship between efficiency and frequency. The maximum efficiency of the two methods is obtained at the resonant frequency. This efficiency is reduced when deviation occurs from the resonant frequency. The efficiency of method 2 is higher than that of method 1, which increases by 0.2% at the resonant frequency and then decreases slowly. This experimental result is in agreement with the simulation.

4.2. Axial deviation-efficiency

Three cases exist in the axial deviation, which are lateral (x axis), forward (y axis), and vertical (z axis) deviations. In experimental method 1, the transmitting and receiving coils are in parallel with each other. In experimental method 2, the receiving coil is parallel with the transmitting coil of the longitudinal pair.

1. Lateral deviation (x axis)

In method 1, the centers of the coils are displaced in the horizontal direction, which is termed lateral deviation. The coil spacing is kept fixed at 12.5 cm, and the lateral deviation ranges from 0 cm to 10 cm. The measurement results in Fig. 7b show that the efficiency decreases with the increase of lateral deviation. This

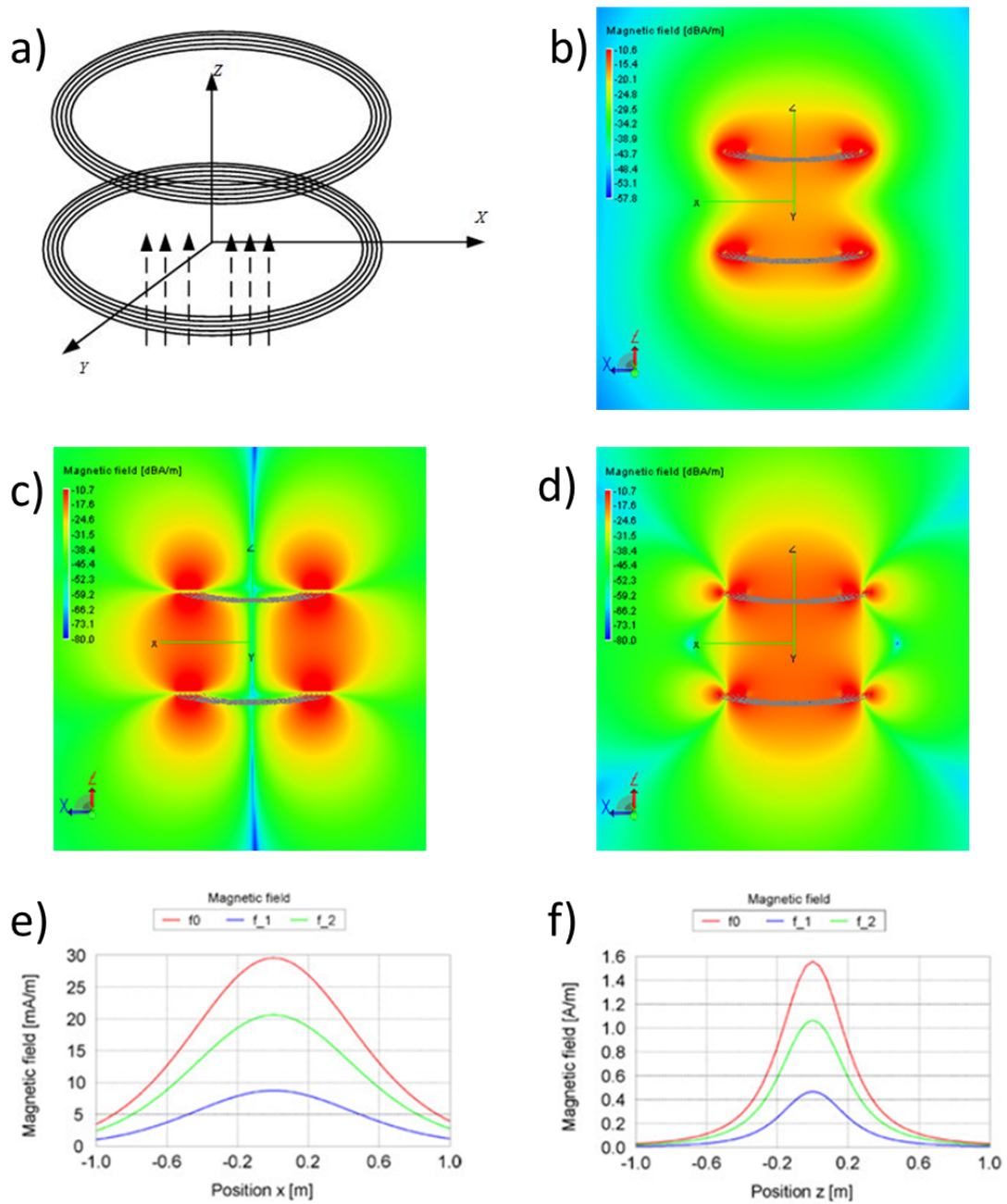


Figure 5: Magnetic field intensity of planar Spiral transmitting coil: a) planar spiral coil, b) general distribution of the magnetic field density, c) x axis component of the magnetic field density distribution, d) z axis component of the magnetic field density distribution, e) Magnetic field intensity along the x axis at different frequencies, f) Magnetic field intensity along the z axis at different frequencies

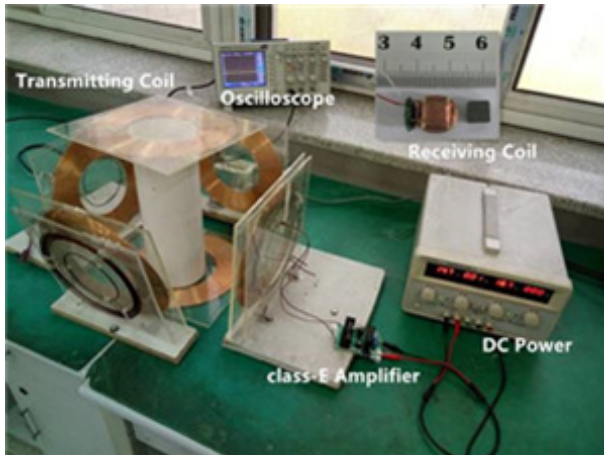


Figure 6: The wireless power supply experimental device for endoscopes

decrement in efficiency is due to the reduction in mutual inductance, which is inversely proportional to deviation. In method 2, the central point of the transmitting coil space is considered the original point, and the axial deviation represents the distance of the transmitting and receiving coils along the axis of the transverse pair. Fig. 7b shows that in the course of the lateral deviation, the power transmission efficiency is improved significantly by using method 2. The results show that the maximum and minimum receiving powers are 790 and 310 mW, respectively, which satisfy the needs of endoscopy power.

The lateral deviation is defined in method 2. As a result, the efficiency decreases greatly when method 1 is used to transmit power, with an increase in the axial and orientation deviations of the power-receiving coil. However, by applying method 2, the power transmission efficiency is improved significantly, especially in the course of the deviation of the orientation. Owing to the irregularity of the same Helmholtz coils, the efficiency decreases but is still higher than the value of method 1. In wireless power transmission, the power applied to the three pairs of power-transmitting coils is variable, because the amplitudes of the energizing currents of the coils are regulated to synthesize the optimal magnetic field vector. The maximum applied power of power-transmitting coils is 35 W, and the power-receiving coil in the capsule can receive steady power of 490 mW.

2. Forward deviation (y axis)

Forward deviation is similar to lateral deviation in which the receiving coil moves along the y axis. Fig. 7c illustrates that the transmission efficiency of method 2 is better than that of method 1. The efficiency of 5 cm is raised from 0.59% to 1.15%. When the y axis is shifted to 10 cm, the efficiency of method 1 is almost zero, and the efficiency of method 2 remains at 0.7%.

3. Vertical deviation (z axis)

In methods 1 and 2, the centers of both coils are located along the same axis. The coil separation distance

can be varied by keeping the transmitter coil fixed while moving the receiver coil along the z axis. For this experiment, the input and output powers are measured, and the separation distance varies from 0 cm to 20 cm.

The experimental result in Fig. 7d shows that the overall efficiency first increases and then decreases with an increase in distance in method 1. The efficiency of method 1 reaches the maximum value at 5 cm and reduces by 0.2% every 2 cm when deviation occurs along the z axis and falls to 0 at 20 cm. The efficiency of method 2 constantly ranges from 1.45% to 2.2% and maintains high efficiency.

4.3. Angular misalignment-efficiency

Fig. 7e shows a plot of power transfer efficiency versus angular misalignment when the receiver is rotated from 0° to 90° for both methods 1 and 2. In this case, the centers of the two coils are kept along the same axis, and the distance to the bottom coil is 12.5 cm in both methods. In method 1, the power transmission efficiency is observed as θ is increased, and the output voltage drops due to the reduction in mutual inductance, which is inversely proportional to θ . When the planes of the coils become orthogonal to each other ($\theta = 90^\circ$), the output is zero. With the application of method 2, the power transmission efficiency is improved significantly. The efficiency increases when the angle deflection is more than 45° because of the six coils.

4.4. Load resistance-efficiency

In this case, the receiving coil is placed on z axis at a fixed distance of 5 cm in method 1 and is placed on the transmitting coil center in method 2. Fig. 7f shows the relationship between load resistance and transmission efficiency.

The load resistance varies from 1Ω to $1 \text{ M}\Omega$. In the experiment, efficiency changes with the variation of load resistance. When the transmission distance is certain, the energy efficiency largely depends on the load resistance in two methods, but a high mutual inductance or coupling coefficient should be applied to achieve a high conversion efficiency in method 2. Efficiency reaches the maximum value when the load impedance is the square of the quality factor of the receiving coil impedance. When the load resistance is $2.7 \text{ k}\Omega$, the maximum efficiency of the two methods is 12.3% and 14.1%. The analysis shows that the transmission distance is certain, and different load resistances have the best access mode to guarantee the maximum transmission efficiency.

5. Conclusions

In this study, a new method for optimizing the efficiency of wireless power transmission suitable for capsule endoscope application was presented. The new method used six transmitting Helmholtz coils with spiral structures, and the coupling coefficient was optimized through electromagnetic localization and synthesis of magnetic field vector. The main conclusions are drawn as follows:

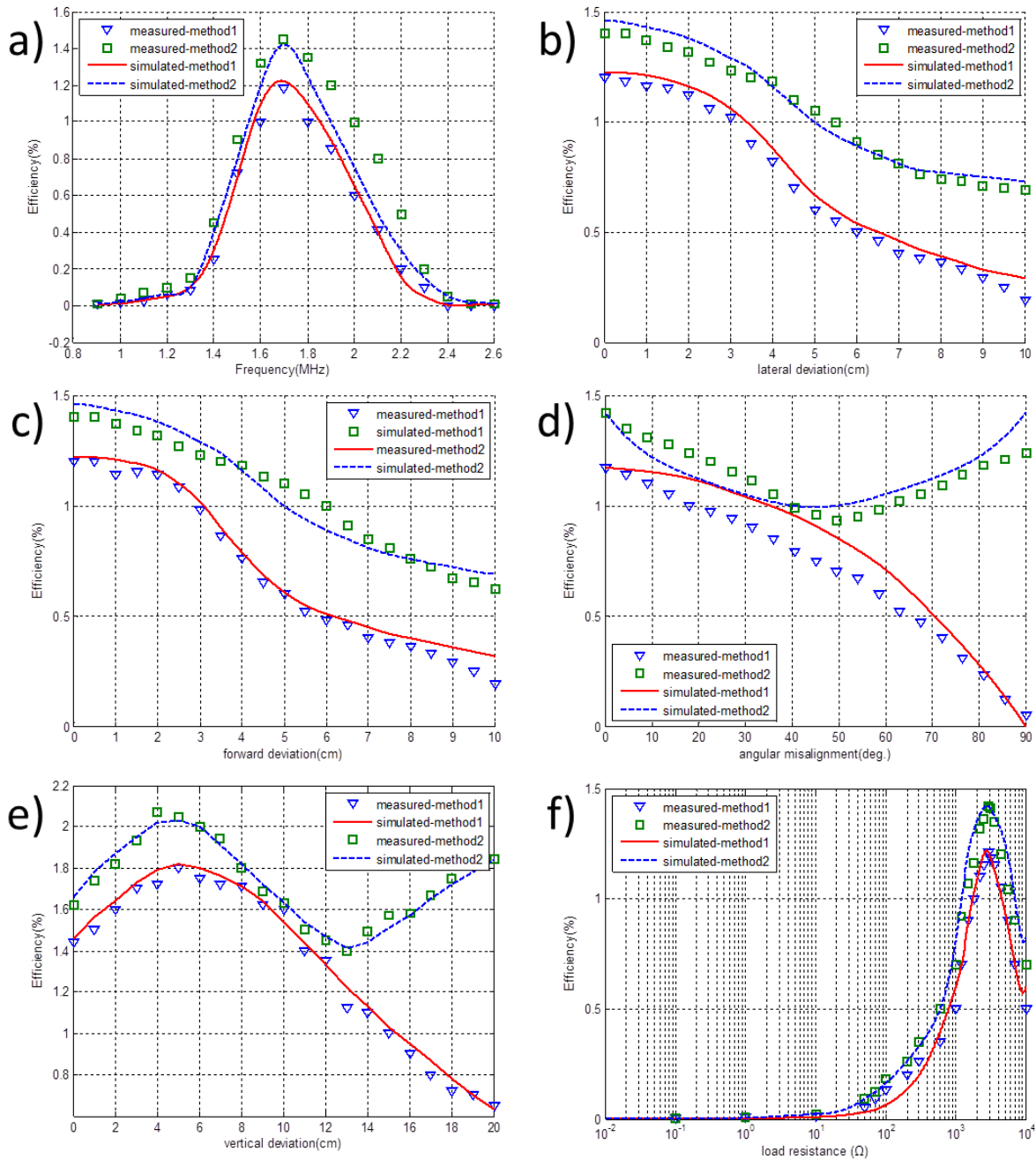


Figure 7: Simulated and Measured Transfer Efficiency of Different Methods: a) frequencies-efficiency, b) lateral (x axis)-efficiency, c) forward (y axis)-efficiency, d) vertical (z axis)-efficiency, e) angular misalignment-efficiency, f) load resistance-efficiency

1. In the magnetic field distribution, method 2 was more uniform with a larger intensity compared with method 1. Thus, the intensity of the magnetic field and the distribution range of the transmitting end were enhanced. Similarly, the transmission power and transmission efficiency were improved effectively. The measurement results showed that the maximum efficiency of the new method was improved from 1.8% to 2.05%.
2. In the distance change situation, the efficiency ranged from 1.42% to 2.05% using the proposed method. When the distance between the transmitting and receiving coils was 12.5 cm in the lateral deviation situation, the efficiency was kept between 0.75% and 1.41%; in the angle misalignment situation, the efficiency was kept between 0.95% and 1.42%.
3. If the maximal applied power of the power-transmitting coils in vitro is 35 W, then the power-receiving coil in the capsule can receive a minimum power of 263 mW at a distance of 12.5 cm, which is sufficient to meet the needs of the endoscope.
4. The transmission efficiency of system changes with the load. When the coil distance is fixed, an optimal load system exists, thereby improving the system maximum transmission efficiency. Different resistance loads have the best access mode and guarantee maximum transmission power and efficiency. Therefore, selecting the load access mode to improve the system transmission power and transmission efficiency is reasonable.

As a result, the method proposed in this article for improving the wireless power transmission efficiency of a capsule endoscope can supply enough power to the capsule regardless of the capsule's orientation and position in the power-transmitting coils. However, in view of the complexity of the wireless transmission and the application of the internal body, future efforts should be directed toward further optimization and miniaturization of the system and further improvement of the practical application of the system.

References

- [1] J. S. Cunha, M. Coimbra, P. Campos, J. M. Soares, Automated topographic segmentation and transit time estimation in endoscopic capsule exams, *Medical Imaging*, IEEE Transactions on 27 (1) (2008) 19–27.
- [2] J. Gao, Traveling magnetic field for homogeneous wireless power transmission, *Power Delivery*, IEEE Transactions on 22 (1) (2007) 507–514.
- [3] A. Moglia, A. Menciassi, M. O. Schurr, P. Dario, Wireless capsule endoscopy: from diagnostic devices to multipurpose robotic systems, *Biomedical Microdevices* 9 (2) (2007) 235–243.
- [4] A. Kurs, A. Karalis, R. Moffatt, J. D. Joannopoulos, P. Fisher, M. Soljačić, Wireless power transfer via strongly coupled magnetic resonances, *science* 317 (5834) (2007) 83–86.
- [5] S. Deb, S.-J. Tang, T. L. Abell, S. Rao, W.-D. Huang, S. F. To, C. Lahr, J.-C. Chiao, An endoscopic wireless gastrostimulator (with video), *Gastrointestinal endoscopy* 75 (2) (2012) 411–415.
- [6] K. M. Silay, C. Dehollain, M. Declercq, A closed-loop remote powering link for wireless cortical implants, *Sensors Journal*, IEEE 13 (9) (2013) 3226–3235.
- [7] S. Kim, J. S. Ho, L. Y. Chen, A. S. Poon, Wireless power transfer to a cardiac implant, *Applied Physics Letters* 101 (7) (2012) 073701.
- [8] A. K. RamRakhyani, S. Mirabbasi, M. Chiao, Design and optimization of resonance-based efficient wireless power delivery systems for biomedical implants, *Biomedical Circuits and Systems*, IEEE Transactions on 5 (1) (2011) 48–63.
- [9] R. Puers, R. Carta, J. Thoné, Wireless power and data transmission strategies for next-generation capsule endoscopes, *Journal of Micromechanics and Microengineering* 21 (5) (2011) 054008.
- [10] B. Lenaerts, R. Puers, An inductive power link for a wireless endoscope, *Biosensors and Bioelectronics* 22 (7) (2007) 1390–1395.
- [11] M. Q. Nguyen, P. Woods, Y.-S. Seo, S. Rao, J. Chiao, Position and angular misalignment analysis for a wirelessly powered stimulator, in: *Microwave Symposium Digest (IMS)*, 2013 IEEE MTT-S International, IEEE, 2013, pp. 1–3.
- [12] W. Wu, Q. Fang, Design and simulation of printed spiral coil used in wireless power transmission systems for implant medical devices, in: *Engineering in Medicine and Biology Society, EMBC, 2011 Annual International Conference of the IEEE*, IEEE, 2011, pp. 4018–4021.
- [13] M. Q. Nguyen, Z. Hughes, P. Woods, Y.-S. Seo, S. Rao, J.-C. Chiao, Field distribution models of spiral coil for misalignment analysis in wireless power transfer systems, *Microwave Theory and Techniques*, IEEE Transactions on 62 (4) (2014) 920–930.
- [14] H. Li, G. Yan, P. Gao, A method for improving the wireless power transmission efficiency of an endoscopic capsule based on electromagnetic localization and synthesis of magnetic field vector, *Proceedings of the Institution of Mechanical Engineers, Part C: Journal of Mechanical Engineering Science* 224 (7) (2010) 1463–1471.
- [15] W. Wang, S. Hemour, K. Wu, Coupled resonance energy transfer over gigahertz frequency range using ceramic filled cavity for medical implanted sensors, *Microwave Theory and Techniques*, IEEE Transactions on 62 (4) (2014) 956–964.
- [16] T. P. Duong, J.-W. Lee, Experimental results of high-efficiency resonant coupling wireless power transfer using a variable coupling method, *Microwave and Wireless Components Letters*, IEEE 21 (8) (2011) 442–444.
- [17] A. P. Sample, D. A. Meyer, J. R. Smith, Analysis, experimental results, and range adaptation of magnetically coupled resonators for wireless power transfer, *Industrial Electronics*, IEEE Transactions on 58 (2) (2011) 544–554.
- [18] H. Hoang, S. Lee, Y. Kim, Y. Choi, F. Bien, An adaptive technique to improve wireless power transfer for consumer electronics, *Consumer Electronics*, IEEE Transactions on 58 (2) (2012) 327–332.